Turk J Chem
31 (2007) , 659 – 666.

Synthesis and Characterization of $NiFe_2O_4$ Nano-Octahedrons by EDTA-Assisted Hydrothermal Method

Nermin KASAPOĞLU[1], Abdulhadi BAYKAL[1*], Muhammet S. TOPRAK[2], Yüksel KÖSEOĞLU[3], Harun BAYRAKDAR[4],

[1] *Department of Chemistry, Fatih University, Büyükçekmece, 34500 İstanbul-TURKEY*
e-mail: hbaykal@fatih.edu.tr

[2] *Department of Chemistry, University of California, Santa Barbara, CA 93106, USA*

[3] *Department of Physics, Fatih University, Büyükçekmece, 34500 İstanbul-TURKEY*

[4] *Department of Physics, Gebze Institute of Technology, 41400 Kocaeli-TURKEY*

Received 27.12.2006

Octahedral-like $NiFe_2O_4$ ferrite nanocrystals were synthesized using EDTA-assisted hydrothermal method under mild conditions. XRD and FTIR analysis were used for composition and structure investigation. XRD analysis revealed a pure ferrite phase with high crystallinity. Morphological investigation by SEM showed octahedral nanocrystals with an average particle size of ∼40 nm. Crystallite size calculated from XRD peak broadening resulted in an average crystallite size of 39 nm, matching well with the SEM observations. TEM analysis and corresponding electron diffraction confirmed the octahedral morphology and single crystallinity of octahedral nanoparticles. Magnetic measurements showed that $NiFe_2O_4$ octahedrons have smaller coercivity than bulk ferrite due to the low shape anisotropy.

Key Words: Octahedral nanocrystals, ferrites, magnetic nanoparticles, hydrothermal synthesis, coercivity, EDTA, $NiFe_2O_4$.

Introduction

Ferrospinel compounds are a very important group of magnetic materials due to their extensive use in a wide range of applications from low to high permeability devices including electronics, ferrofluid, magnetic drug delivery microwave devices, and high density information storage devices.[1−5] They have the general formula of AFe_2O_4 (where A: Fe, Co, Ni, etc.) and a unit cell contains 32 O-atoms in a cubic close packing with 8 Td (tetrahedral) and 16 Oh (octahedral) occupied sites. Among the ferrospinels, the inverse type is

*Corresponding author

particularly interesting due to its high magnetocrystalline anisotropy, high saturation magnetization, and unique magnetic structure.[6]

Nickel ferrite ($NiFe_2O_4$) is an inverse spinel in which half of the ferric ions fill the tetrahedral sites (A-sites) and the rest occupy the octahedral sites (B sites). Thus, the compound can be represented by the formula $(Fe^{3+}_{1.0})[Ni^{2+}_{1.0}Fe^{3+}_{1.0}]O^{2-}_4$, where the round and the square brackets represent A and B sites, respectively.[7] $NiFe_2O_4$ is used in applications including high density magnetic recording media, magnetic refrigeration, magnetic liquids, microwave absorber, and repulsive suspension for leviated railway systems, as catalysts for the benzoylation of toluene with benzyl chloride and gas sensing capabilities towards low concentrations of chlorine gas.[8,9]

$NiFe_2O_4$ exhibits unusual physical and chemical properties when its size is reduced into the nano-region. The solid state reaction method has been conventionally used for the synthesis of nickel ferrites. There are some disadvantages of this technique, such as higher operating temperatures, inhomogeneity of the product, poor stoichiometry, and larger crystallite size. All of the listed qualities have a strong influence on its magnetic properties. To overcome these problems, wet chemical routes, such as sol-gel, combustion, and polyol synthesis are investigated for the synthesis of nano-crystalline oxide powders. Owing to the extremely small dimensions of nano-structured materials, a major portion of the atoms lie at the grain boundaries, which in turn is responsible for superior magnetic, dielectric, and mechanical properties in these materials compared to their conventional coarse grained counterparts.[10–15]

Among the methods that have been used to prepare ferrite nanoparticles,[16–24] the hydrothermal method is one of the abundantly used method because it is economical and has a high degree of compositional control.[25] In addition, the hydrothermal synthesis route does not require extremely high processing temperatures. For example, ferrites can be prepared via the hydrothermal method in the temperature range of 120-160 °C, whereas the solid state method requires a temperature of 800 °C.[26] Hydrothermal synthesis of several ferrites has been reported earlier;[27–29] however, there is no report on the synthesis of octahedral $NiFe_2O_4$ nanocrystals using an EDTA-assisted hydrothermal method. Therefore, our work focuses on the synthesis and comprehensive characterization of octahedral $NiFe_2O_4$ nanocrystals using the EDTA-assisted hydrothermal method.

Experimental

Instruments

The structural characterization was performed using a Huber JSO-DEBYEFLEX 1001 X-ray Diffractometer (XRD) with Cu K_α radiation operated at 40 kV and 35 mA.

FTIR spectra were obtained on a Mattson Satellite Infrared Spectrometer on samples diluted with KBr.

Scanning electron microscopy (SEM) analysis was performed in order to investigate the microstructure and morphology of the sample using a FEI XL40 Sirion FEG digital scanning microscope. Samples were coated with gold at 10 mA for 2 min prior to SEM analysis.

Transmission electron microscopy (TEM) analysis was performed using a Philips-FEI Tecnai G2 T20 at 200 kV accelerating voltage in order to investigate the morphology and crystallinity of synthesized nanoparticles.

Magnetic measurements were performed by the Quantum design vibrating sample magnetometer

(VSM). The magnetization behavior of the synthesized material was scanned in the magnetic field range of 0 to 16 T at different temperatures.

Synthesis

Nanocrystals of $NiFe_2O_4$ were prepared through an EDTA-assisted hydrothermal process. EDTA (0.5 g) was dissolved in 50 mL of distilled water (S1). The starting aqueous solution (S2) of $FeCl_3{\cdot}6H_2O$ and $NiCl_2$ (Ni/Fe mole ratio of 1:2) were prepared by dissolving respective chemicals in S1 under strong mechanical stirring. An aqueous solution of 4.4 M NaOH (S3) was introduced dropwise into S2 solution in a Teflon-lined autoclave under continuous mechanical stirring. The addition of S3 was stopped at pH 12 where a black precipitate formed. The autoclave was then placed in an oven and kept at 160 °C for 15 h. Afterwards, the autoclave was allowed to cool down to room temperature by natural convection. The product was then washed several times with distilled water and absolute ethanol, followed by drying at 100 °C under vacuum for 3 h (Figure 1).

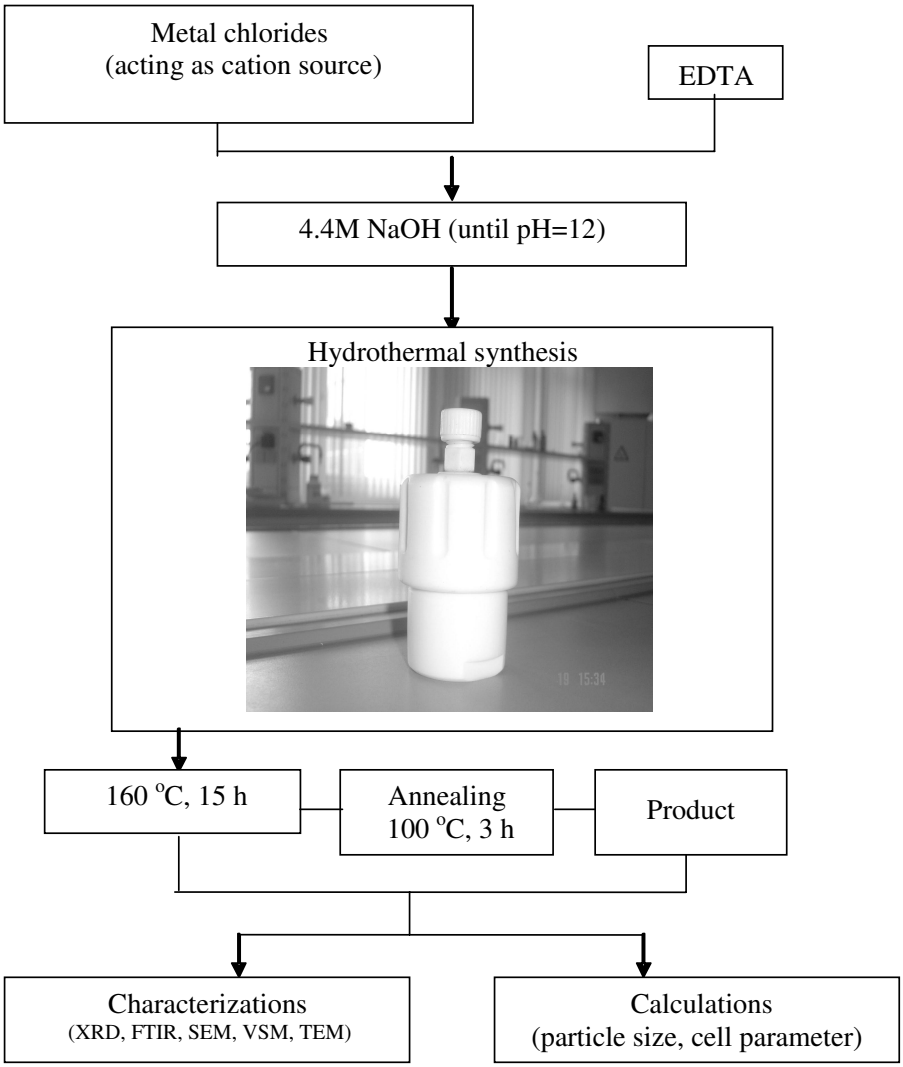

Figure 1. Flow chart of experimental procedure.

Results and Discussion

EDTA plays a crucial role in the formation of octahedral crystals (a strong coordinating agent) by acting as a hexadentate ligand and wrapping itself around the metal ion with 6 suitable positions (4 oxygen atoms and 2 nitrogen atoms). The formation of the complex reduces the concentration of free Fe^{3+} and Ni^{2+} in the solution, and slows down the reaction rate. These are the conditions that are favorable for the growth of octahedral $NiFe_2O_4$ nanocrystals in our synthesis scheme. The proposed scheme has been confirmed earlier on $CoFe_2O_4$ crystals by Zhang et al.[30] They also obtained $CoFe_2O_4$ with irregular shape in the absence of EDTA, or when other coordinating agents such as ethanolamine, ethylenediamine, or pyridine were used. Our findings, as supported by Zhang et al., on similar systems confirm the significance of the presence of EDTA on the formation of octahedral nanocrystals.

XRD Studies

Structural characterization of the final product was performed by X-ray powder diffraction analysis. The XRD pattern is shown in Figure 2 and exhibits typical reflections of (220), (311), (222), (400), (422), (511) and (440) planes that are indications of the presence of the cubic spinel structure. These diffraction lines provide clear evidence on the formation of $NiFe_2O_4$. All of the diffraction peaks match well with the reported values (JCPDS file No:10-325) and are indexed with the lattice parameter of a = 8.339 ± 1 Å. No secondary phase was detected in XRD, ensuring the phase purity of the final product.

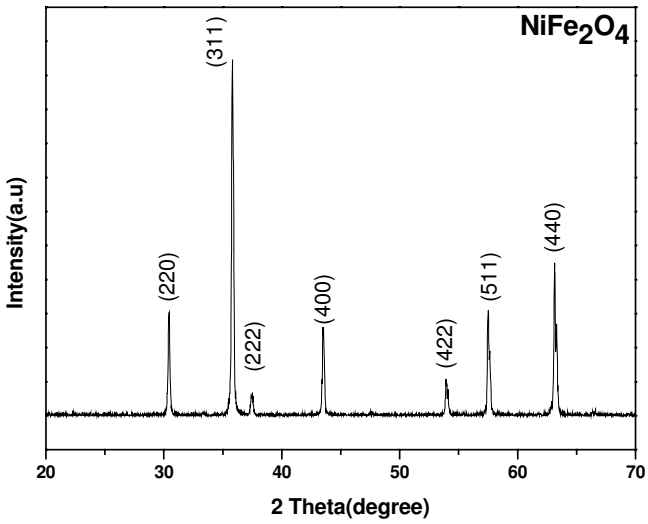

Figure 2. XRD pattern of EDTA-assisted hydrothermally synthesized $NiFe_2O_4$ nanocrystals.

The average crystallite diameter L was estimated by the Scherrer equation using the peak broadening (FWHM) of the most intense peak (3 1 1):

$$L = 0.9\,\lambda \,/\, \beta\cos\theta_B$$

where λ is the wavelength of CuK_α (1.54059 Å), θ_B is the angle of Bragg diffraction, and $\beta = B - b$. Here B is the full width at half maximum (FWHM) and b represents the instrumental line broadening.[31,32] Based on this equation, average crystallite size was calculated as ∼39 nm.

FTIR Studies

FTIR spectra of pure EDTA and nickel ferrite nanocrystals synthesized by the use of EDTA as capping agent are given in Figure 3. Typical bands observed for EDTA are exhibited by the nickel ferrite nanocrystals synthesized via EDTA-assisted hydrothermal route. The band observed at 1694 cm^{-1} for EDTA originates from the free carboxylic groups. A similar band is observed for nickel ferrite nanoparticles capped with EDTA at 1629 cm^{-1}, with a slight shift to lower wavenumbers.[33] It is expected that carboxyl groups will shift to lower wavenumbers when bound to surfaces. Intrinsic stretching vibrations of the metal at the tetrahedral site, $M_{tetra} \leftrightarrow$O, v_1, are generally observed in the range of 620-550 cm^{-1}. Octahedral-metal stretching vibrations, $M_{octa} \leftrightarrow$O,[34–36] v_2-lowest band, are generally observed in the range of 450-385 cm^{-1}.[37] In Figure 3, v_1 stretching vibration of ferrite was observed at 603 cm^{-1} and v_2 stretching vibration was observed around 450 cm^{-1} for the spinel structure.

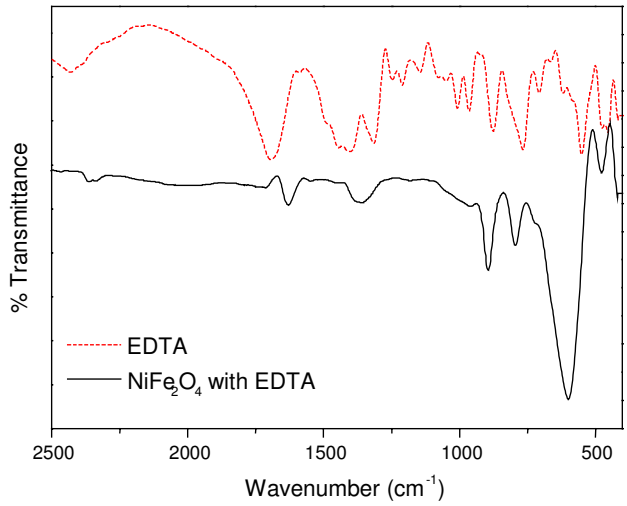

Figure 3. FTIR spectrum of pure EDTA and EDTA-assisted hydrothermally synthesized $NiFe_2O_4$ nanocrystals.

SEM and TEM Studies

SEM was used in order to investigate the morphology of the product and a micrograph is given in Figure 4. A broad size distribution is observed, which consists of nearly octahedral crystals with an average size of about 40 nm. The facets of the octahedrons are apparently distinguishable as further revealed by the circles in Figure 4.

TEM analysis was also performed to confirm the observed morphology of nickel ferrite nanoparticles synthesized by the use of EDTA as a capping agent; a micrograph is presented in Figure 5. Particles exhibited various sizes in the range of 40-80 nm. Nanoparticles mostly in the form of square and paralelloids, as well as their truncated forms, were observed. These observed planes corresponded to the central plane of the octahedral crystals. Selected area electron diffraction pattern (SAED) was taken on one of the crystals and showed a single crystalline diffraction spot that was indexed as [440] planes in the spinel structure; image shown in Figure 5 inset.

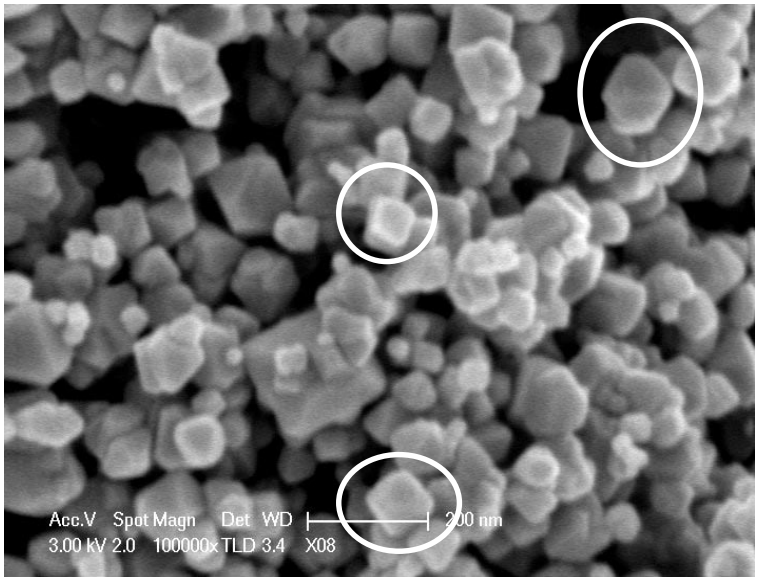

Figure 4. SEM micrograph of EDTA-assisted hydrothermally synthesized $NiFe_2O_4$ nanocrystals.

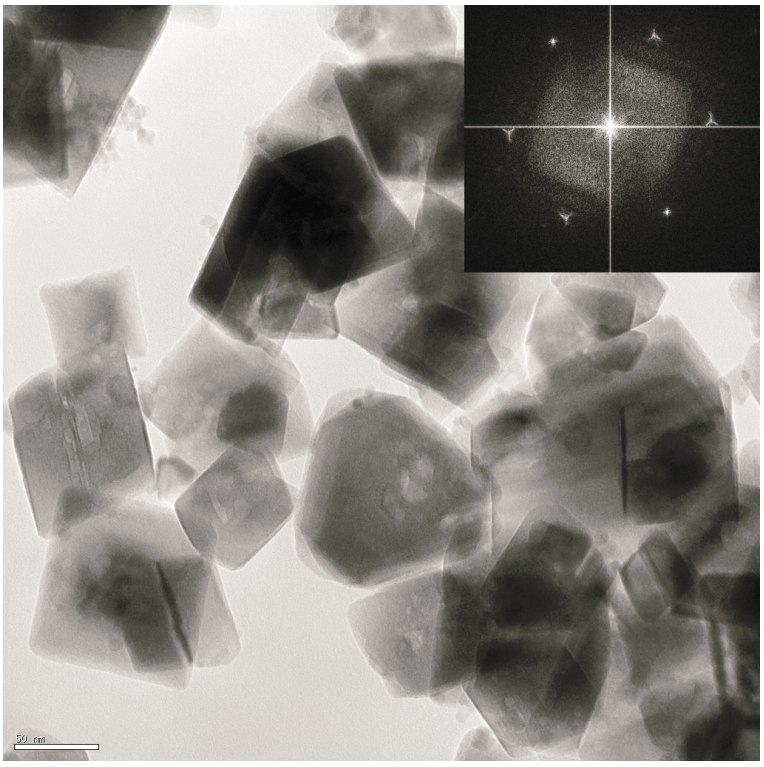

Figure 5. TEM micrograph and electron diffraction pattern of EDTA-assisted hydrothermally synthesized $NiFe_2O_4$ nanocrystals.

Magnetization Studies

Figure 6 shows the typical hysteresis loops for the $NiFe_2O_4$nanoparticles at room temperature and at 10 K, respectively. Octahedral $NiFe_2O_4$ nanocrystals exhibited coercivity ($\boldsymbol{H}_c$) of 70 Oe at room temperature and

541 Oe at 10 K. The room temperature coercivity is less than that of the bulk ferrite.[38] This may be due to the low shape anisotropy and multiple domains of $NiFe_2O_4$ octahedrons, which allow them to magnetize in directions along their easy magnetic axes.

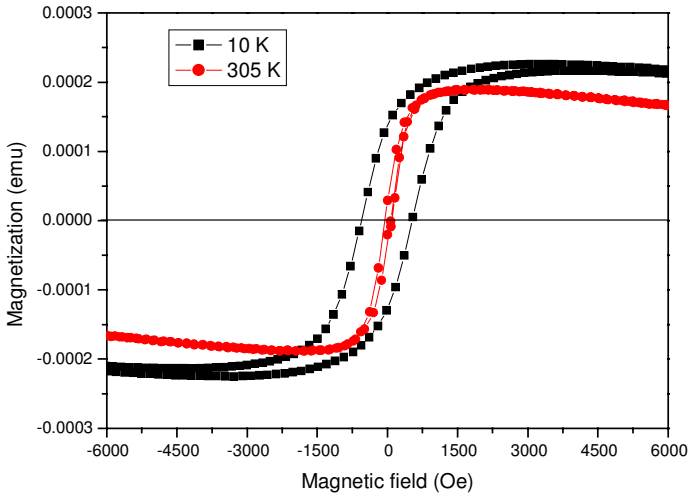

Figure 6. M-H (magnetization-hysteresis) loops of EDTA-assisted hydrothermally synthesized $NiFe_2O_4$ nanocrystals.

Conclusion

Single-phase, well-crystallized octahedral nanocrystals of nickel ferrite were successfully synthesized via an EDTA-assisted hydrothermal method. XRD analysis revealed the high purity of $NiFe_2O_4$. The FTIR spectrum exhibited v_1 and v_2 fundamental bands, corresponding to octahedral and tetrahedral sites in the ferrite structure. Nanocrystals exhibited octahedral morphology as observed from SEM. Average crystallite size calculated from Scherrer equation as ∼39 nm agrees well with the SEM estimated average particle size of 40 nm. This is a good indication of each particle being a single crystal. TEM analysis and corresponding electron diffraction revealed that each octahedral particle is a single crystal. The coercivity of octahedral $NiFe_2O_4$ nanocrystals is lower than that of the bulk ferrite due to the low shape anisotropy.

Acknowledgments

The authors are grateful to the Fatih University Research Project Foundation (Contract no: P50020502) for financial support and Dr. M.S. Toprak acknowledges the fellowship from the Knut and Alice Wallenbergs Foundation (No: UAW2004.0224).

References

1. Y. Qu , H. Yang, N. Yang, Y. Fan, H. Zhu, and G. Zou, **Mater. Lett. 60**, 3548-3522 (2006).
2. P.C. Dorsey, P. Lubitz, D.B. Chrisey, and J.S. Horwitz, **J. Appl. Phys. 85,** 6338-6345 (1999).

3. M.H. Sousa and F.A. Tourinho, **J. Phys. Chem. B 105,** 1168-1175 (2001).
4. F. Mazaleyrat and L.K. Varga, **J. Magn. Magn. Mater. 215**, 253-259 (2000).
5. D.E. Speliotis, **J. Magn. Magn. Mater. 93,** 29-35 (1999).
6. Y. Cheng, Y. Zheng, Y. Wang, F. Bao and Y. Qin, **J. Solid State Chem. 178**, 2394-2397 (2005).
7. M.A. Gabal, **J. Phys. Chem. Solids 64**, 1375-1385 (2003).
8. C.G. Ramankutty and S. Sugunan, **Appl. Catal. A 218**, 39-51 (2001).
9. C.V.G. Reddy, S.V. Manorama and V.J. Rao, **Sens. Actuators B: Chemical 55,** 90-95 (1999).
10. Z.H. Zhou, J.M. Wang, H.S.O. Chan, T. Yu and Z.X. Shen, **J. Appl. Phys. 91**, 6015-6020 (2002).
11. I.E. Candlish, B.H. Kear and B.K. Kim, **Nanostuct. Mater. 1,** 119-124 (1992).
12. G. Skandan, H. Hahn, M. Roddy and W.R. Cannon, **J. Am. Ceram. Soc. 77,** 1706-1710 (1994).
13. M. Kishimoto, Y. Sakurai and T. Ajima, **J. Appl. Phys. 76,** 7506-7509 (1994).
14. Q. Chen and Z.J. Zhang, **Appl. Phys. Lett. 73**, 3156-3158 (1998).
15. S. Music, S. Popovic and S. Dalipi, **J. Mat. Sci. 28**, 1793-1798 (1993).
16. R.N. Singh, N.K. Singh and J.P. Singh, **Electrochim. Acta 47**, 3873-3879 (2002).
17. X.H. Yang, X. Wang and Z.D. Zhang, **J. Cryst. Growth 277**, 467-470 (2005).
18. Y. Sui, D.P. Xu, F.L. Zheng and W.H. Su, **J. Appl. Phys. 80**, 719-723 (1996).
19. A.H. Morrish and K.J. Haneda, **Appl. Phys. 52**, 2496-2498 (1981).
20. A. Bee, R. Massart and S.J. Neveu, **J. Magn. Magn. Mater. 149**, 6-9 (1995).
21. H.F. Yu and A.M. Gadalla, **J. Mater. Res. 11**, 663-670 (1996).
22. T. Pannaparayil, R. Marande and S.J. Komarneni, **J. Appl. Phys. 75**, 1245-1249 (1994).
23. N. Moumen, P. Veillet and M.P. Pileni, **J. Magn. Magn. Mater. 149**, 67-71 (1995).
24. C.L. Huang and E. Matijevic, **Solid State Ion. 84**, 249-258 (1996).
25. N.S. Kommareddi, M. Tata, V.T. John, G.L. McPherson, M.F. Herman and Y.S. Lee, **Chem. Mater. 8**, 801-809 (1996).
26. R.H. Kodama, A.E. Berkowitz and E.J. Mcniff, **Phys. Rev. Lett. 77**, 394-397 (1996).
27. J. Wang, Q. Chen, B. Hou and Z. Peng, **Eur. J. Inorg. Chem. 6**, 1165-1168 (2004).
28. Q. Song and Z.J. Zhang, **J. Am. Chem. Soc. 126**, 6164-6168 (2004).
29. M.M. Bucko and K. Haberko, **J. Eur. Ceram. Soc. 27**, 723-727 (2007).
30. D.E. Zhang, X.J. Zhang, X.M. Ni, J.M. Song and H.G. Zheng, **J. Magn. Magn. Mater. 305**, 68-70 (2006).
31. K.P. Chae, J. Lee, H.S. Kweon and Y.B. Lee, **J. Magn. Magn. Mater. 283**, 103-108 (2004).
32. N. Gupta, A.Verna, S.C. Kashyap and D.C. Dube, **J. Magn. Magn. Mater. 308**, 137-142 (2007).
33. Z. Li, H. Chen and M. Gao, **Chem. Mater. 16**, 1391-1393 (2004).
34. Y. Ahn, E.J. Choi, S. Kim and H.N. Ok, **Mater. Lett. 50**, 47-52 (2001).
35. N. Hanh, O.K. Quy, N.P. Thuy, L.D. Tung and L. Spinu, **Physica B 327**, 382-384 (2003).
36. H.M. Zaki and S.F. Mansour, **J. Phys. Chem. Sol. 67**, 1643-1648 (2006).
37. S. Rana, A. Gallo, R.S. Srivastava and R.D.K. Misra, **Acta Biomater. 3**, 233-242 (2007).
38. X. Huang and Z. Chen, **J. Magn. Magn. Mater. 280**, 37-43 (2004).